RSC Advances

ROYAL SOCIETY OF CHEMISTRY

www.rsc.org/advances

Journal Name

ARTICLE

MALDI-TOF MS and ESI-LTQ-Orbitrap tandem mass spectrometry reveal specific porphyranase activity from *Pseudoalteromonas atlantica* bacterial extract

Received 00th January 20xx,
Accepted 00th January 20xx

DOI: 10.1039/x0xx00000x

www.rsc.org/

C. Przybylski,[a,b] G. Correc,[c] M. Fer,[c†] F. Gonnet,[a b] W. Helbert,[c†*] and R. Daniel[a,b*]

A better understanding of the chemical-physical properties of porphyran – a complex anionic polysaccharide – and the development of potential industrial applications requires more in-depth knowledge of its structural organization. The structural complexity of the hybrid (co-polymer) structure of porphyran stems from the co-occurrence of two repetition moieties LA–G and L6S–G, which can be methylated on the D–Galactose. The enzymes currently available for the structural analyses of porphyran are limited in specificity, and methylated porphyran cannot be digested by previously described β-porphyranases. Here, MALDI-TOF MS analysis and tandem ESI-MS sequencing of porphyran degradation products after incubation with protein extracts from the marine bacterium *Pseudoalteromonas atlantica* revealed methylated disaccharide (L6S–GMe) and dimethylated tetrasaccharide (L6S–GMe–L6S–GMe) end-products that have never been described before. Our results highlighted unprecedented β-methyl-porphyranase activity that can accommodate the methylated building blocks of porphyran.

1. Introduction

Porphyran is a water-soluble agaran belonging to the sulfated galactans family, which also includes carrageenans.[1-4] Sulfated galactans are linear sulfated polysaccharides extracted from the cell wall of red algae and are widely used for industrial applications in the food, cosmetic, and pharmaceutical sectors.[1, 5-13] Like carrageenans, agarans are hybrid polysaccharides composed of several disaccharide repetition moieties, but they differ stereoisometrically: the galactan backbone of carrageenans ($(D–G)_n$) is made exclusively of D–Galactose residues alternately linked by α(1→3) and β(1→4) glycosidic bonds, whereas in agarans ($(L–G)_n$), the α-linked galactose belongs to the L-series.[14-16] The disaccharide repetition moieties can vary in the substitution occurring on the free hydroxyl groups. These substitutions are generally ester sulfate (S) and a 3,6 anhydro-ring (DA or LA) on the 4-linked residue.[14, 17, 18] Other substitutions such methyl (Me) or pyruvate groups (P) also increase the number of possible carrageenan or agaran structures.[17-19] For example, agarose refers to a polysaccharide composed essentially of LA–G (agarobiose) repetition moieties, but also contain methylated and sulfated moieties, whose amounts depend on the algal source and the method of extraction.[20]

Porphyran is extracted from the cell wall of red algae belonging to the genus *Porphyra*, which includes one of the most highly consumed red algal species.[21] The structural complexity of this polysaccharide is due to the co-occurrence of two repetition moieties LA–G and L6S–G, which can be methylated on the [β-linked] D–Galactose giving rise two other repetition moieties: LA–GMe and L6S–GMe (Scheme 1).[17, 22] LA–G is formed *in vivo* from the biosynthetic precursor L6S–G via galactose-6-sulfurylase, and it can also be produced *in vitro* by alkaline treatment of L6S–G.[23, 24] The L6S–G moieties are very abundant in porphyran and are also present in most untreated agarans.

The hybrid (co-polymer) structure of porphyran was first demonstrated by enzymatic degradation with β-agarase[25-27] and more recently with β-porphyranase A.[17] Agarases specifically target the LA–G moieties, which represent about 30% of porphyran[25, 28] whereas β-porphyranases accommodate sulfated L6S–G moieties in their active site.[17, 29] Degradation of agarose repetition units is well documented and numerous enzymes leading to complete saccharification have been described.[30-32] These enzymes include α- and β-agarases, α-3,6-anhydrogalactosidase and β–Galactosidase. In contrast, only a few enzymes that digest segments of L6S–G units have been observed and biochemically characterized. β-porphyranase A and B from the marine bacterium *Zobellia galactinivorans* belonging to the GH16 family of glycoside hydrolases (www.cazy.org) have been studied by enzymology and crystallography thereby depicting the sub-site topology of the active site as well as their substrate specificity.[29] In particular, methylated porphyran cannot be digested by β-porphyranases suggesting that enzymatic digestion of the methylated fraction of porphyran requires other enzymes.

[a] *CNRS, UMR 8587, Laboratoire Analyse et Modélisation pour la Biologie et l'Environnement, F-91025 Evry France*
[b] *Université Evry-Val-d'Essonne, Laboratoire Analyse et Modélisation pour la Biologie et l'Environnement, F-91025 Evry, France.*
[c] *Université Pierre et Marie Curie, Paris VI, Végétaux Marins et Biomolécules, CNRS UMR 7139, Station biologique de Roscoff, 29680 Roscoff, France.*
† Present address: Centre de Recherches sur les Macromolécules Végétales, Equipe Chimie et Biotechnologie des Oligosaccharides, UPR CNRS 5301, 38041 Grenoble Cedex, France.
* regis.daniel@univ-evry.fr; william.helbert@cermav.cnrs.fr

Electronic Supplementary Information (ESI) available: Table S1 list of oligosaccharides detected by MALDI-TOF MS produced by a *Pseudoalteromonas atlantica* protein extract; Text S1, Fig. S1 and Table S2, MALDI-TOF MS analysis of porphyran oligosaccharides produced by β-porphyranase A; Text S2 and Fig. S2 sequencing of β-porphyranase A oligosaccharides using negative ESI-MS^n.

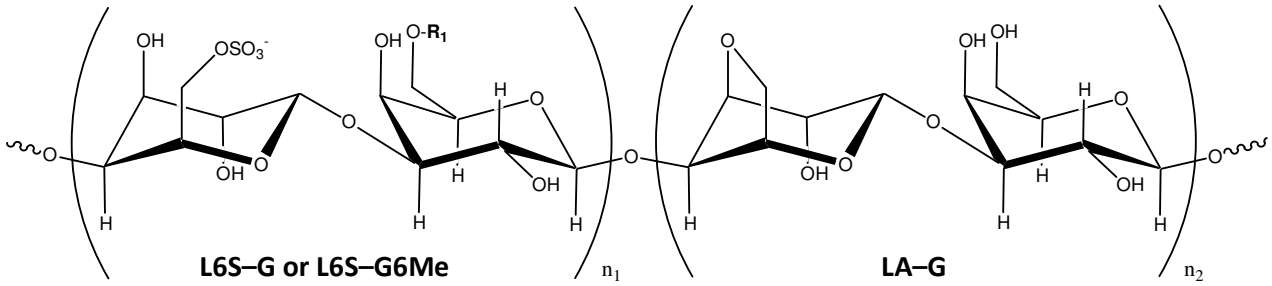

R_1 = H or CH_3; n_1 = number of porphyran disaccharide units; n_2 = number of agarose disaccharide units.

Scheme 1. Chemical structure of the disaccharide building blocks occurring in porphyran. G = D–Galactose, G6Me = 6-O-Methyl D–Galactose, L = L–Galactose, L6S = 6-O-Sulfate L–Galactose, LA = 3,6- anhydro-L–Galactose

Compared to the diversity of other classes of carbohydrate-active enzymes such as the κ-, ι- and λ-carrageenases, the enzymes available for the structural analysis of porphyran are limited in specificity.

Recent genomic and metagenomic investigations of a large variety of biological sources indicate that there is a huge untapped reservoir of new polysaccharide-degrading enzymes, especially porphyranases.[33] Investigation of gene clusters in *Z. galactanivorans*, which correspond to polysaccharide-utilizing loci likely dedicated to the degradation of marine polysaccharides, have led to the identification of new porphyranases.[34] Interestingly, proteins homologous to these bacterial porphyranases have been found in Japanese samples of the human intestinal microbiome. These enzymes were probably acquired after gene transfer from the marine strain present in food made with *Porphyra* sp. (e.g. sushi) through horizontal gene transfer from marine bacteria to human gut bacteria.[33]

We previously implemented a screening method adapted to the detection of polysaccharide-degrading enzymes in complex protein extracts from various marine bacterial strains.[35] Combined with mass spectrometry (MS), this screening method is a powerful tool for the structural analysis of carbohydrate degradation products.[36] Here, we report detailed MS analyses of degradation products obtained after incubation of porphyran with protein extracts from the marine bacterium *Pseudoalteromonas atlantica* (strain T6c).[37] The detailed MS characterization of the resulting oligosaccharides revealed unprecedented series of oligo-porphyran end-products that resulted from heretofore undocumented porphyranase activity.

2. Experimental

2.1 Materials.

2–(4-hydroxyphenylazo)benzoic acid (HABA) and 1,1,3,3-tetramethylguanidine (TMG) were purchased from Sigma-Aldrich Co. (Saint-Quentin-Fallavier, France). HPLC–Grade methanol was obtained from VWR (West Chester, PA, USA). Water was of ultrapure quality, obtained from a MilliQ apparatus (Millipore, Milford, USA). Porphyran was extracted from the red alga *Porphyra umbilicalis* and showed the same chemical features as those previously published.[17]

2.2 Porphyran depolymerization by purified β-porphyranase A.

Porphyran oligosaccharides were obtained by the enzymatic degradation of *P. umbilicalis* porphyran catalyzed by the recombinant β-porphyranase A from *Z. galactanivorans* expressed in *Escherichia coli*,[38] according to a previously described protocol.[17] Briefly, purified porphyran (1% w/v in deionized water) was incubated for 12 h at 30 °C with pure β-porphyranase A (0.15 $\mu g.mL^{-1}$). The completion of the enzyme reaction was ensured by the addition of extra β-porphyranase A (0.15.$\mu g\ mL^{-1}$). The reaction was stopped by heat inactivation (10 min) of the enzyme. Progress of enzymatic depolymerization was monitored by means of reducing-end measurements using a method adapted from Kidby and Davidson,[39] and analytical SEC as previously described.[17] Porphyran oligosaccharides were purified by preparative SEC using three Superdex 30 (26/60) (GE Healthcare) columns in series, integrated in a high-performance liquid chromatography (HPLC) system liquid injector/collector and monitored by Unipoint software (Gilson). The freeze-dried hydrolysis product was dissolved in deionized water at 4% (w/v), and filtered through a 0.45 µm syringe filter (Millipore). Then, 4 mL samples were loaded onto Superdex 30 columns. Detection was carried out by refractive index measurement (Spectra System RI- 50) and 50 mM ammonium carbonate [$(NH_4)_2CO_3$] was used as a running buffer at 1.5 $mL.min^{-1}$ flow rate. Fractions of oligosaccharides were pooled according to their degree of polymerization and subsequently freeze-dried. Oligosaccharide samples were diluted ten-fold either in water for matrix-assisted laser desorption/ionization-time of flight MS (MALDI-TOF MS) analysis or in 1:1 water:methanol (v/v) for electrospray ionization MS (ESI-MS) analysis.

2.3 Porphyran depolymerization by a protein extract from Pseudoalteromonas atlantica.

Pseudoalteromonas atlantica T6c was grown at 18 °C in Zobell medium.[40] A preculture was carried out by inoculating frozen cells in 10 mL of Zobell medium in a 100 mL Erlenmeyer

flask. After incubation for 36 h at 18 °C and then shaking at 150 rpm in a New Brunswick incubator, 1 mL of the culture was inoculated in 50 mL of fresh Zobell medium and incubated for a further 8 h under the same conditions. Then, 50 mL was inoculated in 1 L of Zobell medium under the same conditions (18 °C, 150 rpm, 5 L shaker flask). After 48 h, the culture was centrifuged at 5000 ×g for 30 min at 4 °C. Culture medium was collected and underwent several filtration steps as described in Fer *et al*. .[35] First, filtration through a 300 kDa cut-off membrane was carried out to remove high-molecular-weight macromolecules and cell debris. Then, the filtrate was diafiltered on a 10 kDa cut-off membrane using 100 mM Tris buffer pH 7.5 to eliminate low-molecular-weight molecules (e.g. free sugars). The protein extracts, which contained molecules of molecular weight comprised between 10 kDa and 300 kDa, were incubated with porphyran (0.1% w/v in deionized water) for 20 h at 34 °C. The reaction mixture was then filtered through a 10 kDa cut-off membrane to separate and recover low-molecular-weight oligosaccharides in the filtrate. Oligosaccharide samples were diluted two-fold either in water for MALDI-TOF MS analysis or in 1:1 water:methanol (v/v) for ESI-MS analysis.

2.4 MS analysis.

MALDI-TOF MS experiments were performed using a PerSeptive Biosystems Voyager-DE Pro STR MALDI-TOF mass spectrometer (Applied Biosystems/MDS Sciex, Foster City, CA). This instrument was equipped with a nitrogen UV laser (λ=337 nm) pulsed at a 20 Hz frequency. The mass spectrometer was operated in both the positive and negative ion reflector mode with an accelerating potential of 20 kV and a grid percentage equal to 70%. Mass spectra were recorded with the laser intensity set just above the ionization threshold (2700 in arbitrary units, on our instrument) to avoid fragmentation and labile group losses, to maximize the resolution (pulse width 3 ns) and to obtain a strong analyte signal with minimal matrix interference. Time delay between laser pulse and ion extraction was set to 300 ns. Mass spectra were typically obtained by accumulation of 200-300 laser shots in reflector mode and processed using Data Explorer 4.0 software (Applied Biosystems). The HABA/TMG_2 ionic liquid used as the matrix was prepared as described elsewhere.[41-43] Briefly, HABA was mixed with TMG at a 1:2 molar ratio in methanol. The solution was then sonicated for 15 min at 40 °C. After removal of methanol by centrifugal evaporation in a SpeedVac for 3 h at room temperature, the ionic liquid matrix (ILM) was left under vacuum overnight. Final solutions were then prepared at a concentration of 90 $mg.mL^{-1}$ in methanol and used as a matrix without further purification. Once prepared, these solutions of ILMs can be stored at 4 °C up to 1 week. A 1:1 (v/v) mixture of oligosaccharide sample:ILM was prepared, and 1 µl of the mixture was loaded on a polished stainless steel MALDI target and allowed to dry at room temperature and atmospheric pressure for 5 min.

ESI-MS experiments were carried out on a LTQ-Orbitrap XL from Thermo Scientific (San Jose, CA, USA) and operated in negative ionization mode, with a spray voltage at -5 kV. A 1:1 water:methanol (v/v) mixture was continuously infused using a 250 µL syringe at 10 $µL.min^{-1}$ flow. Applied voltages were - 35 and - 110 V for the ion transfer capillary and the tube lens, respectively. The ion transfer capillary was held at 275 °C. Resolution was set to 60 000 (at m/z 400) for all experiments, and the m/z ranges were set to 300-2000 in profile mode and in the normal mass range during full-scan experiments. Spectra were analyzed using the acquisition software XCalibur 2.0.7 (Thermo Scientific, San Jose, CA, USA), without smoothing or background subtracts. During MS/MS scans, collision-induced dissociation (CID) fragmentation occurred in the linear ion-trap analyzer and detection in Orbitrap with centroid mode. For CID fragmentation, an activation Q value (Q) of 0.25 and an activation time (T) equal to 30 ms were used. Normalized collision energy (NCE) was set at 25% for MS/MS experiments and 15-25% for MS^n experiments (with n>2). The automatic gain control (AGC) allowed accumulation up to 1.10^6 ions for Fourier-transform MS (FTMS) scans, 2.10^5 ions for $FTMS^n$ scans and 1.10^4 ions for ion-trap MS ($ITMS^n$) scans. Maximum injection time was set to 500 ms for both FTMS and $FTMS^n$ scans and 100 ms for $ITMS^n$ scans. For all scan modes, 1 µscan was acquired. The precursor selection window was 2 Da and 3 Da during MS^2 and MS^n (with n>2), respectively. Each ion with z ≥2 present in the full-scan MS and exhibiting a signal intensity of >500 arbitrary units was fragmented by iterative $ESI\text{-}MS^n$ steps (with n≥2). Fragments resulting from fragmentation steps were annotated according to the nomenclature described by Domon and Costello.[44]

3. Results and discussion

3.1 Comparison of β-porphyranase A and P. atlantica end-products.

After incubation of a protein extract from the marine bacterium *P. atlantica* with porphyran, MALDI-TOF MS analysis revealed a series of oligosaccharides, thereby indicating that *P. atlantica* possesses porphyranase activity (Figure 1A). The spectrum of the incubation showed a wide distribution of ions ranging from *m/z* 421.07 (dp2) to *m/z* 2815.47 (dp14) (Supporting Information, Table S1) revealing a new, undocumented series of oligo-porphyrans. Mass spectrum of the heat shock inactivated *P. atlantica* extract clearly revealed no ions corresponding to oligosaccharides (data not shown). For comparison, the MALDI mass spectrum of the depolymerization products obtained after digestion of porphyran with purified β-porphyranase A (Figure 1B) exhibited fewer species ranging from *m/z* 421.07 (dp2) to *m/z* 2283.49 (dp12) (Supporting Information, Table S2). The di- and tetrasaccharide end-products formed by β-porphyranase A have been previously characterized by NMR and showed that the disaccharide α-L–Galp-6-sulfate (1→3) ß-D–Galp (L6S–G) is the major end-product and that higher oligosaccharides belong to methylated and non-methylated L6S–G series.[17, 29] Accordingly, the three most intense ions in the mass spectrum of the β-porphyranase A end-products were at *m/z* 421.07,

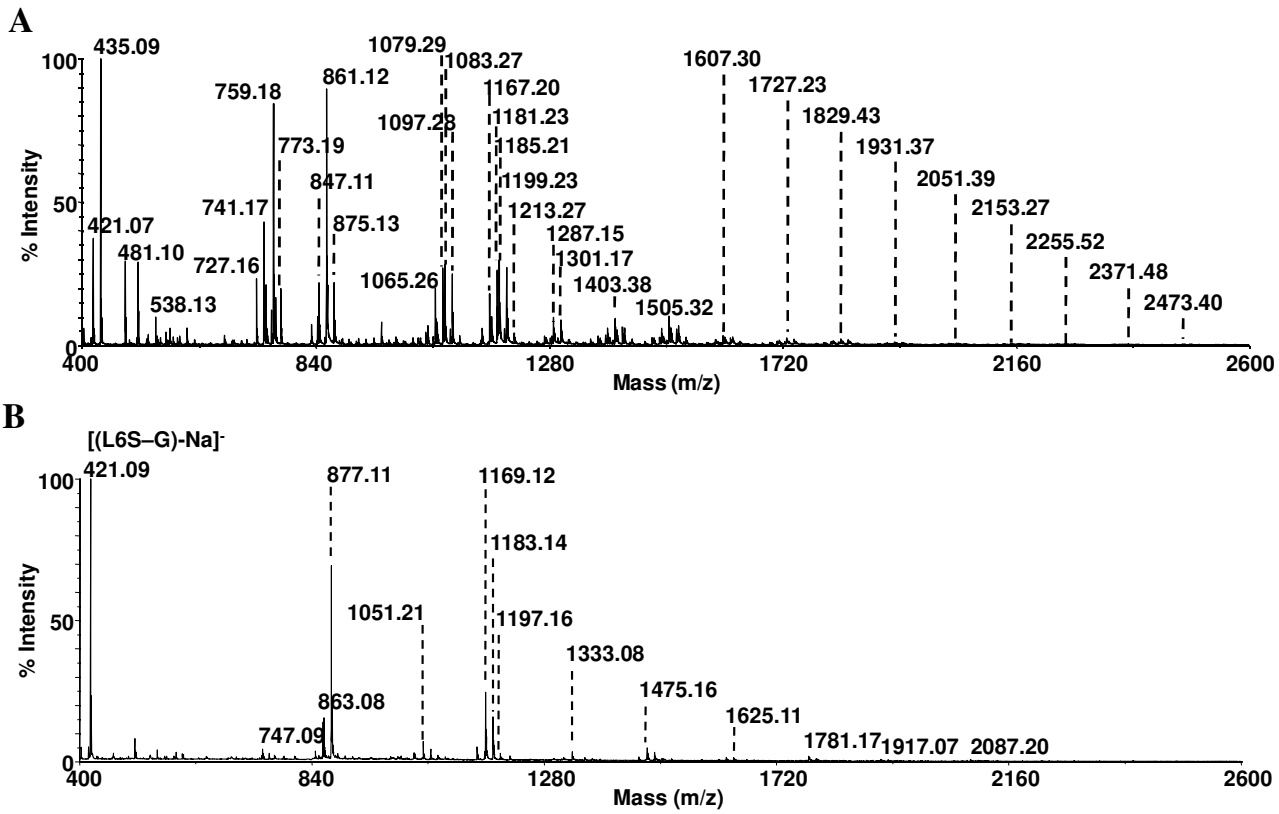

Fig. 1. Negative ion reflector MALDI-TOF mass spectra of porphyran depolymerization reaction mixtures incubated with (A) *Pseudoalteromonas atlantica* protein extract and (B) β-porphyranase A. Fully detailed annotations of the different ions are given in Supporting Information.

877.11 and 1169.12 (Figure 1B) corresponding to the disaccharide L6S–G, a methylated tetrasaccharide (L6S–G)$_2$+CH_3 and a disulfated hexasaccharide including an anhydrogalactose residue (LA–G)(L6S–G)$_2$, respectively. The first striking difference between *P. atlantica* and β-porphyranase A end-products was observed in the range of dp2. The L6S–G (*m/z* 421.07) was the only dp2 limit product produced by β-porphyranase A, whereas the *P. atlantica* extract yielded two dp2 limit products at *m/z* 421.07 (L6S–G) and at *m/z* 435.09 (Figure 1A). The latter dp2 ion was the most intense and was ascribed to a monomethylated disaccharide (L6S–G+CH_3). For higher-molecular-weight oligosaccharides, the number of species was systematically greater for *P. atlantica* extracts than for β-porphyranase A end-products. For example, the dp4 species detected after β-porphyranase A digestion included two oligosaccharides without and with one methyl group (*m/z* at 863.08 and 877.11, respectively) and was based on a (L6S–G)$_2$ backbone (Figure 1B), while at least three monosodiated tetrasaccharides with no *(m/z* 847.11), one (*m/z* 861.12) and two (*m/z* 875.13) methyl groups were observed with the *P. atlantica* extract (Figure 1A). Similarly, the dp6 oligosaccharides detected after β-porphyranase A digestion were based on a [(LA–G)(L6S–G)$_2$-2Na+K]$^-$ backbone with no, one or two methyl groups, while the more diverse backbones ([(LA–G)(L–G)(L6S–G)]$^-$, [(L–G)$_2$(L6S–G)]$^-$, [(LA–G)(L6S–G)$_2$], [(L–G)(L6S–G)$_2$]) were observed for the dp6 oligosaccharides formed by the *P. atlantica* extracts (Supporting Information, Table S1 and S2).

3.2 Sequencing of β-porphyranase A oligosaccharides using ESI-MS^n.

The β-porphyranase A depolymerization products have been previously analyzed by NMR,[17] but they have only been partly characterized by mass spectrometry using a particularly high-energy photon activation,[36] and the location of the methyl groups and the discrimination between several isomers had remained unknown. In this study, end-products of β-porphyranase A were purified by SEC and analyzed using MALDI-TOF revealing slight size heterogeneity in SEC fractions (Table 1, and Supporting Information Text S1 and Figure S1), and ESI MS^n in negative ionization. ESI-MS^n can determine characteristic MS^n fragmentation patterns that were then used to elucidate the new series of oligo-porphyrans produced by the *P. atlantica* extract (Supporting Information Text S2 and Figure S2 for a complete description of the MS^n experiments).

Fragmentation of the dp2 ion at *m/z* 421.0645 led to the formation of a non-reducing end sulfated galactose and fragment ions resulting from intra-cyclic cleavages that established the presence of a sulfate group at the C-6 position of the non-reducing end galactose (Figure S2A). These MS/MS

data confirmed that the dp2 fraction was the monosulfated disaccharide galactosyl–Galactose L6S–G, in full agreement with the typical building block depicted for porphyran.[17] This L6S–G disaccharide appeared to be the limit product of the enzymatic β-porphyranase A depolymerization of porphyran.
The tetrasaccharide SEC fraction contained two disulfated tetrasaccharide species detected as doubly charged ions at *m/z* 412.0583 and *m/z* 419.0663, the latter having a mass increment of 14.0160 mass units corresponding to a methyl group (data not shown). The ESI-MS^2 fragmentation of the disulfated tetrasaccharide ion at *m/z* 412.0583 resulted in cross-ring cleavages and glycosidic bond cleavages leading to non-reducing end mono-, di- and trisaccharides and reducing-end trisaccharides, which together with further MS^3 fragmentations (data not shown) were in agreement with the following porphyran tetrasaccharide sequence: (L6S–G)–(L6S–G) (Supporting Information, Figure S2B). The methylated disulfated tetrasaccharide at *m/z* 419.0663 also underwent ESI-MS^2 and MS^3 fragmentation, in both negative and positive ionizations, and located the methyl group on the second galactose residue from the non-reducing end in the following tetrasaccharide sequence: (L6S–G6Me)–(L6S–G) (Supporting Information, Figure S2C).

Similar MS^n investigations were conducted with the four detected dp6 end-products of β-porphyranase A, which shared a common (L6S–G)–(LA–G)–(L6S–G) backbone but varied according to the occurrence of 0, 1 or 2 methyl groups. Fragmentation of the non-methylated hexasaccharide with its doubly charged ion $[M-2Na]^{2-}$ at *m/z* 565.1051 led to the following sequence: (L6S–G)–(LA–G)–(L6S–G) localizing the anhydro–Galactose (LA) in the central disaccharide (Supporting Information, Figure S2D). Fragmentation of the doubly charged ion $[M-2Na]^{2-}$ at *m/z* 572.1131 corresponding to a monomethylated hexasaccharide revealed that this dp6 ion could be attributed to two hexasaccharide isomers differing in the position of the methyl group. Further MS^n fragmentations (data not shown) located the methyl group on the G unit either in the internal LA–G disaccharide or in the non-reducing end LA–G disaccharide, leading to the following complete sequences of the two isomers: (L6S–G)–(LA–G6Me)–(L6S–G) and (L6S–G6Me)–(LA–G)–(L6S–G) (Supporting Information, Figure S2E). Taking into account the intensity of specific fragment ions for each isomer, we assumed a ≈30:70 ratio for (L6S–G6Me):(LA–G6Me). With regard to the dimethylated hexasaccharide detected at *m/z* 579.1204, its MS^2 fragments indicated that the methyl groups were not located at the reducing-end disaccharide. Further fragmentations delineated the following sequence: (L6S–G6Me)–(LA–G6Me)–(L6S–G) for this fourth hexasaccharide isomer contained in the dp6 fraction (Supporting Information, Figure S2F).

3.3 Characterization of a new series of methylated oligo-porphyrans produced by P. atlantica.

The ESI-MS analysis of the depolymerization products from the *P. atlantica* incubation confirmed the presence of two dp2 limit products as non-methylated and methylated disaccharides detected at *m/z* 421.0635 and at *m/z* 435.0792, respectively (Inset, Figure 2). The ESI-MS^2 fragmentation of the methylated dp2 ion $[M-Na]^-$ at *m/z* 435.0792 in negative ionization mode, as well as in positive ionization mode for its counterpart $[M+H]^+$ positive ion at *m/z* 459.0801, located the sulfate group and the methyl moiety at the C-6 of the L–Galactose (L) unit and at the C-6 of the reducing D–Galactose residue (G), respectively (data not shown), leading to the dp2 structure L6S–G6Me.

Higher dp oligosaccharides showed higher structural diversity than those obtained with β-porphyranase A (Table 2). In addition to the oligo-porphyran dp4 and dp6 already described with β-porphyranase A, new distinct oligosaccharides were detected and characterized. In particular, we observed the occurrence of a dimethylated dp4 as a dicharged ion at m/z 426.0750 (Figure 2). MS/MS experiments yielded a major B_3^{2-} ion at *m/z* 329.0355 corresponding to a disulfated trisaccharide with only one methyl remaining (Figure 3A). It resulted from the glycosidic bond cleavage that released the reducing-end methylated galactose from the parent tetrasaccharide and formed the B_3^{2-} ion $[M_{dp4}–G6Me-2Na]^{2-}$. Two cross-ring fragments at *m/z* 308.0311 ($^{0,2}A_3^{3-}$) and *m/z* 374.0510 ($^{1,4}A_4^{2-}$) confirmed the presence of a methyl group on the C-6 of the reducing-end galactose. Further MS^3 fragmentation experiments targeting the B_3^{2-} ion at *m/z* 329.0355 provided an intense peak at *m/z* 417.0674 (Figure 3B) that corresponded to a monosulfated disaccharide including one methyl group. The peak at *m/z* 417.0674 resulted from the loss of a L6S moiety and was mainly attributed to a B_2 fragment corresponding to a $[M_{dp4}–(L6S–G6Me)-Na]^-$ species. This *m/z* value can also contain a small part of Y_3, but B_2 was favored due to preferential charge localization at the non-reducing end. Other glycosidic bond cleavages were also observed, leading to B_1/C_1 ions at 241.0015/259.0023 and C_2 ion at 435.0788. Two minor cross-ring cleavages at *m/z* 138.9706 ($^{0,4}A_1$) and *m/z* 299.0257 ($^{2,4}X_3^{2-}$), attested to the presence of a sulfate group on the L–Galactose of each disaccharide repeat. Further fragmentations *via* an MS^4 step on the most intense B_2 at *m/z* 417.0674 led to a dominant ion at *m/z* 241.0022 assigned to a B_1 fragment (Figure 3C) corresponding to a sulfated galactose. Taken together, these fragments confirmed the methylation of the G residue located in the third position from reducing end of the tetrasaccharide. MS^5 fragmentation of the B_1 ion (*m/z* 241.0022) led to the loss of sulfate anion at *m/z* 96.9603, and to cross-ring cleavages $^{0,4}A_1$ (*m/z* 138.9708), $^{0,3}A_1$-H_2O (*m/z* 150.9705), $^{0,3}A_1$ (*m/z* 168.9809) and $^{0,4}A_1$-H_2O (*m/z* 180.9808), which unambiguously located the sulfate group at the C-6 of the non-reducing-end galactose. Overall, these iterative MS fragmentations were consistent with the following tetrasaccharide sequence: (L6S–G6Me)–(L6S–G6Me). In addition to a higher degree of methylation, the *P. atlantica* oligosaccharides also showed differences in their methylation pattern. Unlike β-porphyranase A oligosaccharides, a significant part of the detected tetrasaccharides formed by *P. atlantica* were found methylated on the reducing-end galactose (Table 2).

Table 1. Ions detected by MALDI-TOF MS in negative mode after incubation of β-porphyranase A with porphyran and separation by SEC (only ions with ≥1% of the relative abundance are reported). All ions detected within each SEC fraction were listed, and putative oligosaccharide composition (not the sequence) is given.

Fractions	m/z ([M-Na]$^-$)		Mass accuracy (ppm)	Putative composition
	Experimental	Theoretical		
dp2	421.10	421.07	24	[(L6S–G)-Na]$^-$
dp4	583.15	583.15	0	[(G)(L6S–G)-Na]$^-$
	597.13	597.13	0	[(G)(L6S–G)+CH_3-Na]$^-$
	745.17	745.17	0	[(L–G)(L6S–G)-Na]$^-$
	759.19	759.19	0	[(L–G)(L6S–G)+CH_3-Na]$^-$
	847.11	847.11	0	[$(L6S–G)_2$-Na]$^-$
	861.14	861.13	12	[$(L6S–G)_2$+CH_3-Na]$^-$
	863.08	863.08	0	[$(L6S–G)_2$-2Na+K]$^-$
	877.10	877.10	0	[$(L6S–G)_2$+CH_3-2Na+K]$^-$
	1033.25	1033.26	10	[$(LA–G)_2$(L6S–G)-Na]$^-$
	1051.32	1051.31	10	[(LA–G)(L–G)(L6S–G)-Na]$^-$
	1153.22	1153.20	17	[(LA–G)$(L6S–G)_2$-Na]$^-$
dp4-Me	597.13	597.13	0	[(G)(L6S–G)+CH_3-Na]$^-$
	699.06	699.07	14	[(L6S–G)(L6S)+CH_3-Na]$^-$
	745.17	745.17	0	[(L–G)(L6S–G)-Na]$^-$
	759.19	759.19	0	[(L–G)(L6S–G)+CH_3-Na]$^-$
	847.11	847.11	0	[$(L6S–G)_2$-Na]$^-$
	861.13	861.13	0	[$(L6S–G)_2$+CH_3-Na]$^-$
	863.08	863.08	0	[$(L6S–G)_2$-2Na+K]$^-$
	877.11	877.10	11	[$(L6S–G)_2$+CH_3-2Na+K]$^-$
	1051.32	1051.31	10	[(LA–G)(L–G)(L6S–G)-Na]$^-$
	1065.30	1065.28	19	[(LA–G)(L–G)(L6S–G)+CH_3-Na]$^-$
	1153.21	1153.20	9	[(LA–G)$(L6S–G)_2$-Na]$^-$
	1167.23	1167.22	9	[(LA–G)$(L6S–G)_2$+CH_3-Na]$^-$
dp6	745.19	745.17	27	[(L–G)(L6S–G)-Na]$^-$
	759.21	759.19	26	[(L–G)(L6S–G)+CH_3-Na]$^-$
	861.15	861.13	23	[$(L6S–G)_2$+CH_3-Na]$^-$
	1051.31	1051.31	0	[(LA–G)(L–G)(L6S–G)-Na]$^-$
	1065.28	1065.28	0	[(LA–G)(L–G)(L6S–G)+CH_3-Na]$^-$
	1153.20	1153.20	0	[(LA–G)$(L6S–G)_2$-Na]$^-$
	1167.22	1167.22	0	[(LA–G)$(L6S–G)_2$+CH_3-Na]$^-$
	1183.20	1183.19	8	[(LA–G)$(L6S–G)_2$+CH_3-2Na+K]$^-$
dp6-Me	1051.30	1051.31	10	[(LA–G)(L–G)$(L6S–G)_2$-N]$^-$
	1065.28	1065.28	0	[(LA–G)(L–G)(L6S–G)+CH_3-Na]$^-$
	1079.29	1079.30	9	[(LA–G)(L–G)(L6S–G)+2CH_3-Na]$^-$
	1083.29	1083.29	0	[$(L–G)_2$(L6S–G)+CH_3-Na]$^-$
	1153.20	1153.20	0	[(LA–G)$(L6S–G)_2$-Na]$^-$
	1167.22	1167.22	0	[(LA–G)$(L6S–G)_2$+CH_3-Na]$^-$
	1181.25	1181.24	8	[(LA–G)$(L6S–G)_2$+2CH_3-Na]$^-$
	1183.17	1183.19	17	[(LA–G)$(L6S–G)_2$+CH_3-2Na+K]$^-$
	1185.21	1185.23	17	[(L–G)$(L6S–G)_2$+CH_3-Na]$^-$
	1201.19	1201.20	8	[(L–G)$(L6S–G)_2$+CH_3-2Na+K]$^-$
	1213.25	1213.26	8	[(L–G)$(L6S–G)_2$+3CH_3-Na]$^-$
	1215.21	1215.22	8	[(L–G)$(L6S–G)_2$+2CH_3-2Na+K]$^-$
	1303.14	1303.14	0	[$(L6S–G)_3$+CH_3-2Na+K]$^-$
	1317.18	1317.16	15	[$(L6S–G)_3$+2CH_3-2Na+K]$^-$
	1357.34	1357.36	15	[(L–G)$(LA–G)_2$(L6S–G)-Na]$^-$
	1371.36	1371.38	15	[(L–G)$(LA–G)_2$(L6S–G)+CH_3-Na]$^-$
	1375.38	1375.37	7	[(LA–G)$(L–G)_2$(L6S–G)-Na]$^-$
	1459.32	1459.30	14	[$(LA–G)_2$$(L6S–G)_2$-Na]$^-$
	1473.33	1473.32	7	[$(LA–G)_2$$(L6S–G)_2$+$CH_3$-Na]$^-$

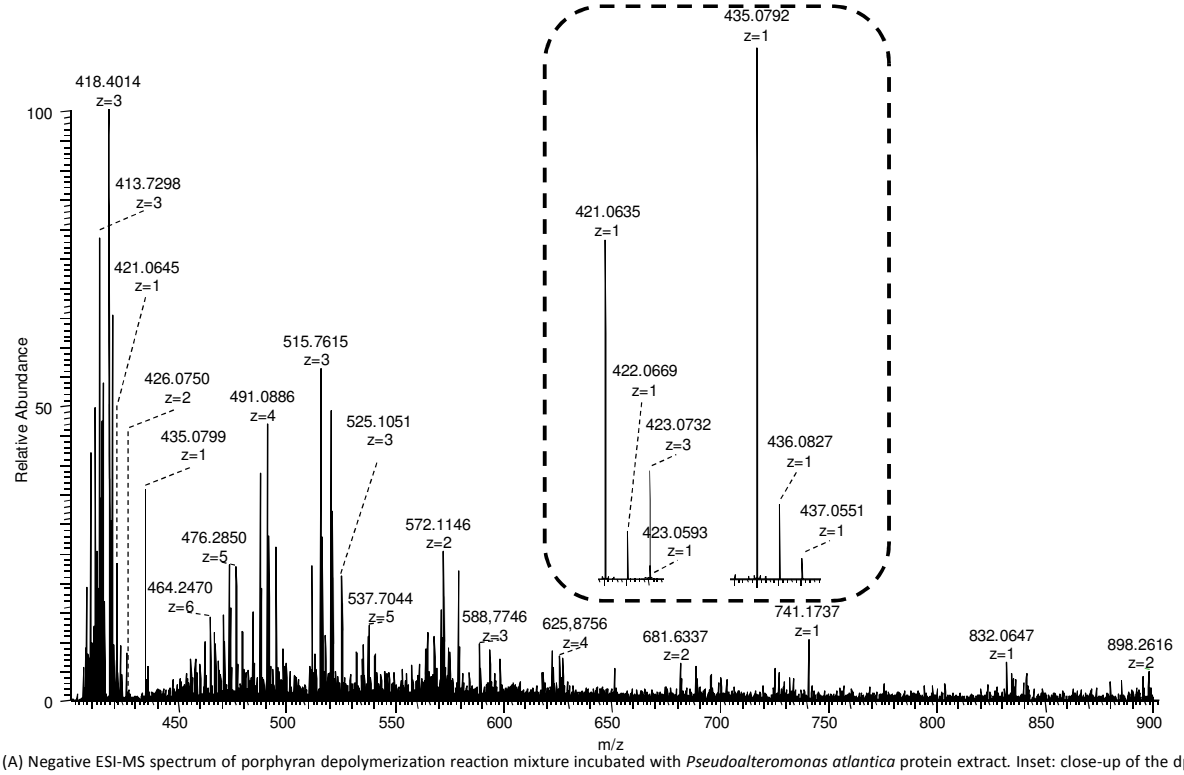

Fig. 2. (A) Negative ESI-MS spectrum of porphyran depolymerization reaction mixture incubated with *Pseudoalteromonas atlantica* protein extract. Inset: close-up of the dp2 *m/z* area pointing to the disaccharide limit products at *m/z* 421.0645 and 435.0799, without and with a methyl group, respectively.

The triply charged species at *m/z* 418.4014 appearing as the most intense ion in the ESI-MS spectrum (Figure 2) was attributed to a porphyran trisulfated hexasaccharide including two methyl groups. Its MS^2 fragmentation yielded a major ion at *m/z* 358.3792 corresponding to a trisulfated pentasaccharide with two methyl groups (Figure 4A). We assume that it resulted from a glycosidic rupture releasing the terminal galactose unit at the reducing end of the parent hexasaccharide thereby forming the B_5^{3-} ion $[M_{dp6}–G\text{-}3Na]^{3-}$. Two cross-ring fragments at *m/z* 388.3895 ($^{1,4}A_6^{3-}$) and *m/z* 579.1199 ($^{2,4}A_6^{2-}$) confirmed the absence of a methyl group on the C-6 of the reducing-end galactose. Nevertheless, an additional B_5^{3-} ion at *m/z* 353.7074 and $^{1,4}A_6^{3-}$ ion at *m/z* 383.7147 was weakly detected, corresponding to a trisulfated pentasaccharide with only one methyl group (underlined ions in Figure 4A). This result indicates that a minor proportion of the parent ions had a methylated galactose (G6Me) at the reducing end, thus highlighting the structural heterogeneity of the parent dimethylated trisulfated hexasaccharide with regard to the location of methyl groups. Other glycosidic bond cleavages of the parent hexasaccharide were also detected at *m/z* 241.0011, *m/z* 417.0683/435.0785, *m/z* 329.0346/338.0398, *m/z* 417.0683/426.0734, *m/z* 364.3825 for B_1, B_2/C_2, B_3^{2-}/C_3^{2-}, B_4^{2-}/C_4^{2-}, C_5^{3-}, respectively from the non-reducing end, and at *m/z* 410.0637/419.0672, *m/z* 498.0943/507.0994 and *m/z* 597.1305 for Z_4^{2-}/Y_4^{2-}, Z_5^{2-}/Y_5^{2-} and Y_3 respectively from the reducing end. Further fragmentation by MS^3 experiments targeting the B_5^{3-} ion at *m/z* 358.3792 provided an intense peak at *m/z* 417.0681 (Figure 4B) that corresponded to a disulfated tetrasaccharide including two methyl groups. It resulted from the loss of a L6S moiety and was attributed to a B_4^{2-} corresponding to $[M_{dp6}–(L6S–G)\text{-}3Na]^{2-}$ species. Another minor B_4^{2-} ion at *m/z* 410.0613 was also observed, corresponding to a disulfated tetrasaccharide with one methyl group $[M_{dp6}–(L6S–G6Me)\text{-}3Na]^{2-}$. Additional glycosidic bond cleavages were observed, one of them yielding the second-most intense ion (55% of the base peak) at *m/z* 329.0345 and attributed to a B_3^{2-} fragment, *i.e.* a disulfated trisaccharide with one methyl group $[M_{dp6}–(G6Me\text{-}L6S–G)\text{-}3Na]^{2-}$. Another B_3^{2-} fragment of lower intensity at *m/z* 322.0263 was also detected corresponding to $[M_{dp6}–(G6Me\text{-}L6S–G6Me)\text{-}3Na]^{2-}$. Subsequent MS^4 dissociation experiments performed on the most intense B_4^{2-} at *m/z* 417.0681 led to two B_3^{2-} fragments (Figure 4C), an intense one at *m/z* 329.0355 corresponding to $[M_{dp6}–(G6Me–L6S–G)\text{-}3Na]^{2-}$, and a minor one at *m/z* 322.0277 as previously observed in the MS^3 step. The MS^4 spectrum revealed also two cross-ring ions at *m/z* 308.0307 ($^{0,2}A_3^{2-}$) and *m/z* 374.0509 ($^{1,4}A_4^{2-}$) that confirmed the methylation of the G residue located in the third position from the hexasaccharide reducing end. Further sequential multistage MS experiments were carried out on the most intense ions, continuing up to MS^7 fragmentation of the non-reducing end terminal residue of the parent hexasaccharide, *i.e.* a sulfated L–Galactose (Figure 4D). This latter residue was produced upon the MS^6 fragmentation of the B_2^- ion corresponding to the non-reducing disaccharide L6S–G6Me (not shown). The MS^7 soft fragmentation of B_1 fragment (m/z 241.0015) mainly produced two singly charged

Table 2. Sequences of oligosaccharides formed after incubation with *Pseudoalteromonas atlantica* extract and determined by ESI-MS^n in negative mode (only ions with ≥1% of the relative abundance are reported). All oligosaccharides have been submitted to the same procedure.

dp	m/z ([M-nNa]$^{n-}$)		Mass accuracy (ppm)	Deduced sequences
	Experimental	Theoretical		
2	421.0645^{1-}	421.0652^{1-}	1.7	L6S–G
	435.0799^{1-}	435.0809^{1-}	2.3	L6S–G6Me
4	727.1594^{1-}	727.1603^{1-}	1.2	LA–G–L6S–G
	741.1750^{1-}	741.1759^{1-}	1.2	LA–G6Me–L6S–G (18%) LA–G–L6S–G6Me (82%)
	755.1903^{1-}	755.1916^{1-}	1.7	LA–G6Me–L6S–G6Me
	412.0593^{2-}	412.0599^{2-}	1.5	L6S–G–L6S–G
	419.0672^{2-}	419.0677^{2-}	1.2	L6S–G6Me–L6S–G (35%) L6S–G–L6S–G6Me (65%)
	426.0750^{2-}	426.0756^{2-}	1.4	L6S–G6Me–L6S–G6Me
6	1033.2549^{1-}	1033.2554^{1-}	0.5	L6S–G–LA–G–LA–G
	1047.2703^{1-}	1047.2710^{1-}	0.7	L6S–G6Me–LA–G–LA–G (45%) L6S–G–LA–G6Me–LA–G (30%) L6S–G–LA–G–LA–G6Me (25%)
	1061.2861^{1-}	1061.2867^{1-}	0.6	L6S–G6Me–LA–G6Me–LA–G (56%) L6S–G6Me–LA–G–LA–G6Me (31%) L6S–G–LA–G6Me–LA–G6Me (13%)
	565.1069^{2-}	565.1075^{2-}	1.1	L6S–G–LA–G–LA–G
	572.1146^{2-}	572.1153^{2-}	1.2	L6S–G6Me–LA–G–L6S–G (39%) L6S–G–LA–G6Me–L6S–G (31%) L6S–G–LA–G–L6S–G6Me (30%)
	579.1225^{2-}	579.1231^{2-}	1.0	L6S–G6Me–LA–G6Me–L6S–G (71%) L6S–G6Me–LA–G–L6S–G6Me (22%) L6S–G–LA–G6Me–L6S–G6Me (7%)
	409.0582^{3-}	409.0582^{3-}	0.0	L6S–G–L6S–G–L6S–G
	413.7297^{3-} - -	413.7300^{3-} - -	0.7	L6S–G6Me–L6S–G–L6S–G (57%) L6S–G–L6S–G6Me –L6S–G (30%) L6S–G–L6S–G–L6S–G6Me (13%)
	418.4012^{3-} - -	418.4019^{3-} - -	1.7	L6S–G6Me–L6S–G6Me–L6S–G (79%) L6S–G6Me –L6S–G–L6S–G6Me (17%) L6S–G–L6S–G6Me–L6S–G6Me (4%)
	423.0732^{3-}	423.0738^{3-}	1.4	L6S–G6Me–L6S–G6Me–L6S–G6Me

Table 2. (continued)

dp	m/z ([M-nNa]$^{n-}$)		Mass accuracy (ppm)	Deduced sequences
	Experimental	Theoretical		
10	484.0812^{4-}	484.0811^{4-}	0.2	$(L6S–G)_4(LA–G)$
	487.5847^{4-}	487.5849^{4-}	0.4	$(L6S–G)_4(LA–G)$+1Me [a)]
	491.0886^{4-}	491.0888^{4-}	0.4	$(L6S–G)_4(LA–G)$+2Me [a)]
	494.5923^{4-}	494.5928^{4-}	1.0	$(L6S–G)_4(LA–G)$+3Me [a)]
	498.0962^{4-}	498.0967^{4-}	1.0	$(L6S–G)_4(LA–G)$+4Me [a)]
12	567.1172^{4-}	567.1178^{4-}	1.1	$(L6S–G)_4(LA–G)_2$+3Me
	574.1255^{4-}	574.1257^{4-}	0.4	$(L6S–G)_4(LA–G)_2$+5Me
	470.2817^{5-}	470.2830^{5-}	2.8	$(L6S–G)_5(LA–G)$+2Me [a)]
	473.0868^{5-}	473.0872^{5-}	0.9	$(L6S–G)_5(LA–G)$+3Me [a)]
	476.8890^{5-}	476.8893^{5-}	0.6	$(L6S–G)_5(LA–G)$+3Me [a)]
	478.7919^{5-}	478.7924^{5-}	1.0	$(L6S–G)_5(LA–G)$+4Me [a)]
14	461.7439^{6-}	461.7441^{6-}	0.4	$(L6S–G)_6(LA–G)$+2Me
	464.0798^{6-}	464.0801^{6-}	0.7	$(L6S–G)_6(LA–G)$+3Me
	529.0951^{5-}	529.0949^{5-}	0.4	$(L6S–G)_5(LA–G)_2$
	531.8975^{5-}	531.8979^{5-}	0.8	$(L6S–G)_5(LA–G)_2$+1Me [a)]
	534.7004^{5-}	534.7010^{5-}	1.1	$(L6S–G)_5(LA–G)_2$+2Me [a)]
	537.5040^{5-}	537.5042^{5-}	0.4	$(L6S–G)_5(LA–G)_2$+3Me [a)]
	540.3076^{5-}	540.3073^{5-}	0.6	$(L6S–G)_5(LA–G)_2$+4Me [a)]
	543.1106^{5-}	543.1104^{5-}	0.4	$(L6S–G)_5(LA–G)_2$+5Me [a)]
	466.4160^{6-}	466.4160^{6-}	0.0	$(L6S–G)_6(LA–G)$+4Me
	468.7524^{6-}	468.7520^{6-}	09	$(L6S–G)_6(LA–G)$+5Me
16	453.3595^{7-}	453.3599^{7-}	0.9	$(L6S–G)_7(LA–G)$+2Me
	455.3620^{7-}	455.3621^{7-}	0.2	$(L6S–G)_7(LA–G)$+3Me
	457.3643^{7-}	457.3644^{7-}	0.2	$(L6S–G)_7(LA–G)$+4Me
	459.3662^{7-}	459.3666^{7-}	0.9	$(L6S–G)_7(LA–G)$+5Me
	512.7602^{6-}	512.7600^{6-}	0.4	$(L6S–G)_6(LA–G)_2$+2Me
	517.4326^{6-}	517.4319^{6-}	1.4	$(L6S–G)_6(LA–G)_2$+4Me [b)]
18	447.0708^{8-}	447.0717^{8-}	2.0	$(L6S–G)_8(LA–G)$+2Me
	448.8234^{8-}	448.8237^{8-}	0.7	$(L6S–G)_8(LA–G)$+3Me
	450.5752^{8-}	450.5757^{8-}	1.1	$(L6S–G)_8(LA–G)$+4Me
	501.0915^{7-}	501.0923^{7-}	1.6	$(L6S–G)_7(LA–G)_2$+4Me
	503.0938^{7-}	503.0945^{7-}	1.4	$(L6S–G)_7(LA–G)_2$+5Me
	505.0958^{7-}	505.0967^{7-}	1.8	$(L6S–G)_7(LA–G)_2$+6Me

[a)]: number of isomers ≥3; [b)] : number of isomers ≥4.

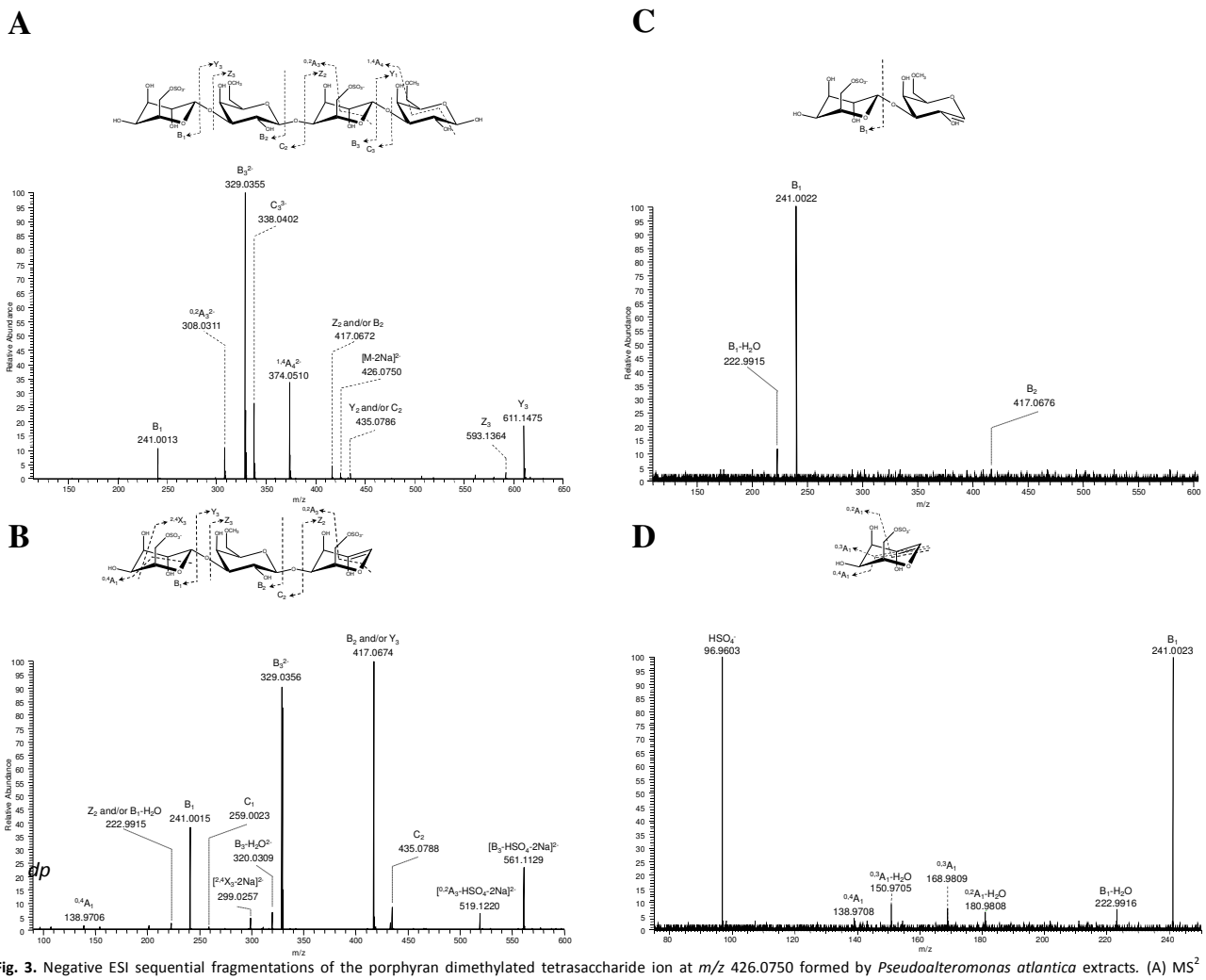

Fig. 3. Negative ESI sequential fragmentations of the porphyran dimethylated tetrasaccharide ion at *m/z* 426.0750 formed by *Pseudoalteromonas atlantica* extracts. (A) MS^2 spectrum of the $[dp4\text{-}2Na]^{2-}$ precursor ion at *m/z* 426.0750. (B) MS^3 spectrum of the B_2^{3-} ion at *m/z* 329.0355. (C) MS^4 spectrum of the B_2 ion at *m/z* 417.0674. (D) MS^5 spectrum of the B_1 ion at *m/z* 241.0022.

ions,at *m/z* 241.0021 and *m/z* 96.9602, corresponding to a remaining B_1 precursor ion attributed to non-reducing end monosaccharide L6S and the sulfate anion HSO_4^-, respectively. Additional ions at *m/z* 138.9706, 150.9706, 168.9811 and 180.9810 resulting from cross-ring cleavages $^{0,4}A_1$, $^{0,3}A_1$-H_2O, $^{0,3}A_1$ and $^{0,4}A_1$-H_2O respectively, unambiguously positioned the sulfate group at the C-6 of the terminal galactose residue. By combining all these MS^n data, we conclude that the parent dimethylated trisulfated hexasaccharide is actually composed of the three following isomers: (L6S–G6Me)–(L6S–G6Me)–(L6S–G), (L6S–G6Me)–(L6S–G)–(L6S–G6Me) and (L6S–G)–(L6S–G6Me)–(L6S–G6Me) (Table 2). Their proportions can be estimated at ≈79, 17 and 4%, respectively, based on the intensity of their fragments and considering similar ionization efficiency of each parent isomer. This ESI-MS^n approach thus provides a complete structural elucidation of various isobaric porphyran oligosaccharides.

4. Conclusion

The Detailed MS sequencing of the degradation products of porphyran incubated with protein extracts from the marine bacterium *P. atlantica* revealed a new series of oligosaccharides that differed markedly in their level of methylation from those obtained with *Z. galactinovorans* β-porphyranase A. The methylated disaccharide (L6S–GMe) and dimethylated tetrasaccharide (L6S–GMe-L6S–GMe) end-products formed by the *P. atlantica* extract have never been observed before and were absent in the end-products of β-porphyranase A. This result suggests that a β-porphyranase with new substrate specificity is present in *P. atlantica* extracts. The occurrence of a methylated disaccharide end-product demonstrated that *P. atlantica* β-porphyranase accommodates at least one methyl group in its active site. Furthermore, the observation of a dimethylated tetrasaccharide indicates that methyl group can be positioned at the reducing or non-reducing ends of the oligosaccharide substrate. Therefore, the active site of this novel enzyme, likely a β-methyl-

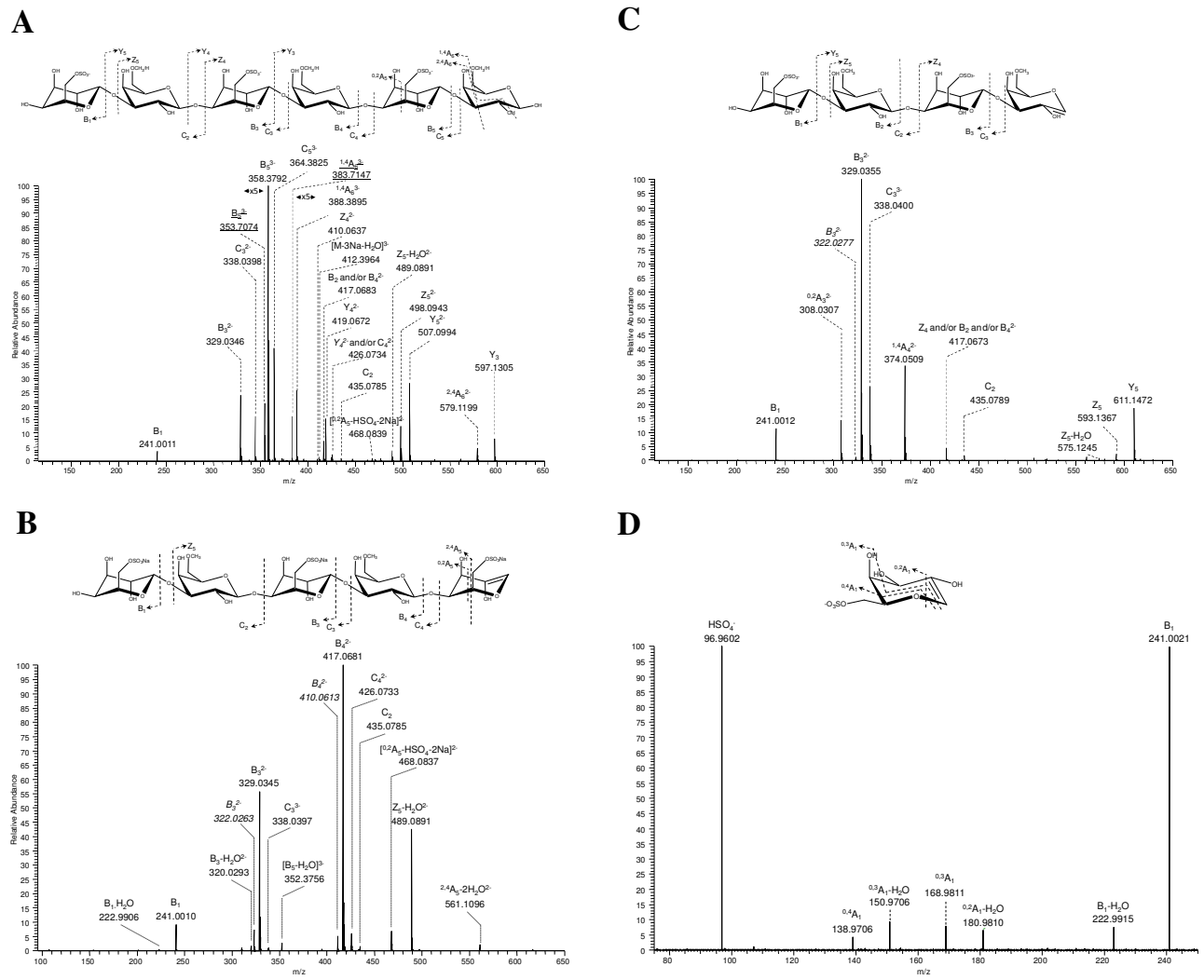

Fig. 4. Negative ESI sequential fragmentations of a dimethylated hexasaccharide fraction formed by *Pseudoalteromonas atlantica* extracts. (A) MS^2 spectrum of the $[dp6\text{-}3Na]^{3-}$ precursor ion at *m/z* 418.4015. (B) MS^3 spectrum of the B_5^{3-} ion at *m/z* 358.3792. (C) MS^4 spectrum of the B_4^{2-} ion at *m/z* 417.0681. (D) MS^7 spectrum of the B_1 ion at *m/z* 241.0021. Fragments attesting to methylation at the non-reducing end are underlined.

porphyranase, can accommodate methylated porphyran and catalyze a cleavage reaction that cannot be performed by previously described β-porphyranases belonging to the GH16 and GH86 glycoside hydrolase families.[29, 38]

This study was conducted using protein extracts that may contain several enzymes involved in the degradation of porphyran; among them, one or several enzymes must have methyl porphyran specificities. Previous inspection of the *P. atlantica* genome revealed that four genes code for a protein belonging to the GH16 family, but one protein *PatI_0824* (Q15XN6, http://www.uniprot.org/uniprot/Q15XN6) in particular showed sequence homology with *Z. galactinovorans* β-porphyranase A.[38] This protein has been cloned and overexpressed in *E. coli* and has similar substrate specificity as *Z. galactinovorans* β-porphyranases A. Therefore, the β-methyl-porphyranase identified here probably has a different protein sequence from previously described porphyranases or belongs to a new glycoside hydrolase family. The isolation and characterization of this new β-methyl-porphyranase is underway.

Given the hybrid structure of porphyran and its numerous chemical modifications such as methylation, porphyranases with a variety of substrate specificities are required for more in-depth knowledge of the polysaccharide's structure. Although there is a high degree of methylation — above 50%[45] — at the C-6 position of the D–Galactose units, the previously described β-porphyranase cannot catalyze glycosidic bond cleavage within methylated sequences. Therefore, the new methyl β-methyl-porphyranase activity described here will be a valuable structural tool and, combined with β-agarases and β-porphyranases, can produce the building blocks specific to porphyrans from various red algal species.

Acknowledgements

The authors sincerely thank Genopole-France and the Île-de-France Regional Council for generous financial support.

References

1. V. H. Pomin and P. A. S. Mourão, *Glycobiology*, 2008, **18**, 1016.
2. S. Knutsen, D. Myslabodski, B. Larsen and A. I. Usov, *Botanica Marina*, 1994, **37**, 163.
3. S. Peat, J. R. Turvey and D. A. Rees, *J. Chem. Soc.*, 1961, DOI: 10.1039/JR9610001590, 1590.
4. S. Peat and D. A. Rees, *Biochem. J.*, 1961, **79**, 7.
5. S. Bhatia, A. Sharma, K. Sharma, M. Kavale, B. Chaugule, K. Dhalwal, A. Namdeo and K. Mahadik, *Phcog. Rev.*, 2008, **2**, 271.
6. G. A. De Ruiter and B. Rudolph, *Trends Food Sci. Tech.*, 1997, **8**, 389.
7. M.-J. Kwon and T.-J. Nam, *Life Sci.*, 2006, **79**, 1956.
8. H. Noda, *J. Appl. Phycol.*, 1993, **5**, 255.
9. D.-H. Ngo and S.-K. Kim, *Int. J. Biol. Macromol.*, 2013, **62**, 70.
10. K. Nisizawa, H. Noda, R. Kikuchi and T. Watanabe, *Hydrobiologia*, 1987, **151-152**, 5.
11. S. Fukuda, H. Saito, S. Nakaji, M. Yamada, N. Ebine, E. Tsushima, E. Oka, K. Kumeta, T. Tsukamoto and S. Tokunaga, *Eur. J. Clin. Nutr.*, 2006, **61**, 99.
12. N. Inoue, N. Yamano, K. Sakata, K. Nagao, Y. Hama and T. Yanagita, *Biosci. Biotech. Bioch.*, 2009, **73**.
13. K. Ishihara, C. Oyamada, R. Matsushima, M. Murata and T. Muraoka, *Biosci. Biotech. Bioch.*, 2005, **69**, 1824.
14. V. L. Campo, D. F. Kawano, D. B. d. Silva Jr and I. Carvalho, *Carbohyd. Polym.*, 2009, **77**, 167.
15. F. van de Velde, *Food Hydrocolloid.*, 2008, **22**, 727.
16. A. I. Usov, *Food Hydrocolloid.*, 1998, **12**, 301.
17. G. Correc, J.-H. Hehemann, M. Czjzek and W. Helbert, *Carbohyd. Polym.*, 2011, **83**.
18. F. van de Velde, S. H. Knutsen, A. I. Usov, H. S. Rollema and A. S. Cerezo, *Trends Food Sci. Tech.*, 2002, **13**, 73.
19. M. Lahaye, W. Yaphe, M. T. P. Viet and C. Rochas, *Carbohyd. Res.*, 1989, **190**, 249.
20. D. A. Rees and E. Conway, *Biochem. J.*, 1962, **84**, 411.
21. Z. A. Popper, G. Michel, C. Hervé, D. S. Domozych, W. G. T. Willats, M. G. Tuohy, B. Kloareg and D. B. Stengel, *Annu. Rev. Plant Biol.*, 2011, **62**, 567.
22. N. S. Anderson and D. A. Rees, *J. Chem. Soc.*, 1965, DOI: 10.1039/JR9650005880, 5880.
23. D. A. Rees, *Biochem. J.*, 1961, **81**, 347.
24. M. D. Noseda, A. G. Viana, M. E. R. Duarte and A. S. Cerezo, *Carbohyd. Polym.*, 2000, **42**, 301.
25. M. Duckworth and J. R. Turvey, *Biochemical J.*, 1969, **113**.
26. L. M. Morrice, M. W. McLean, W. F. Long and F. B. Williamson, *Eur. J. Biochem.*, 1983, **133**.
27. L. M. Morrice, M. W. McLean, W. F. Long and F. B. Williamson, in *Eleventh International Seaweed Symposium*, eds. C. Bird and M. Ragan, Springer Netherlands, 1984, vol. 22, ch. 118, pp. 572-575.
28. J. R. Turvey and J. Christison, *Biochem. J.*, 1967, **105**, 317.
29. J.-H. Hehemann, G. Correc, F. Thomas, T. Bernard, T. Barbeyron, M. Jam, W. Helbert, G. Michel and M. Czjzek, *J. Biol. Chem.* , 2012, **287**.
30. M. Jam, D. Flament, J. Allouch, P. Potin, L. Thion, B. Kloareg, M. Czjzek, W. Helbert, G. Michel and T. Barbeyron, *Biochem. J.*, 2005, **385**, 703.
31. G. Michel, P. Nyval-Collen, T. Barbeyron, M. Czjzek and W. Helbert, *Appl. Microbiol. Biot.*, 2006, **71**.
32. W.-J. Chi, Y.-K. Chang and S.-K. Hong, *Appl Microbiol. Biot.*, 2012, **94**.
33. B. L. Cantarel, P. M. Coutinho, C. Rancurel, T. Bernard, V. Lombard and B. Henrissat, *Nucleic Acids Res.*, 2009, **37**, D233.
34. J.-H. Hehemann, A. G. Kelly, N. A. Pudlo, E. C. Martens and A. B. Boraston, *Proc. Natl. Acad. Sci. U.S.A.*, 2012, **109**, 19786.
35. M. Fer, A. Préchoux, A. Leroy, J.-F. Sassi, M. Lahaye, C. Boisset, P. Nyvall-Collén and W. Helbert, *J. Microbiol. Methods*, 2012, **89**.
36. D. Ropartz, A. Giuliani, C. Hervé, A. Geairon, M. Jam, M. Czjzek and H. Rogniaux, *Anal. Chem.*, 2015, **87**, 1042.
37. R. Belas, D. Bartlett and M. Silverman, *Appl. Environ. Microbiol.*, 1988, **54**, 30.
38. J.-H. Hehemann, G. Correc, T. Barbeyron, W. Helbert, M. Czjzek and G. Michel, *Nature*, 2010, **464**.
39. D. K. Kidby and D. J. Davidson, *Anal. Biochem.*, 1973, **55**.
40. C. E. Zobell, *J. Mar. Res.*, 1941, **4**, 42.
41. C. Przybylski, F. Gonnet, D. Bonnaffé, Y. Hersant, H. Lortat-Jacob and R. Daniel, *Glycobiology*, 2010, **20**.
42. A. Seffouh, F. Milz, C. Przybylski, C. Laguri, A. Oosterhof, S. Bourcier, R. Sadir, E. Dutkowski, R. Daniel, T. H. van Kuppevelt, T. Dierks, H. Lortat-Jacob and R. R. Vivès, *FASEB J.*, 2013, **27**.
43. D. Ropartz, P.-E. Bodet, C. Przybylski, F. Gonnet, R. Daniel, M. Fer, W. Helbert, D. Bertrand, H. Rogniaux and 0., *Rapid Commun. Mass Spectrom.*, 2011, **25**.
44. B. Domon and C. E. Costello, *Glycoconjugate J.*, 1988, **5**, 397.
45. Q. Zhang, H. Qi, T. Zhao, E. Deslandes, N. M. Ismaeli, F. Molloy and A. T. Critchley, *Carbohyd. Res.*, 2005, **340**, 2447.